Nondestructive 3D Pathology Image Atlas of Barrett Esophagus With Open-Top Light-Sheet Microscopy

Deepti M. Reddi, MD; Lindsey A. Barner, MS; Wynn Burke, MS; Gan Gao, BS; William M. Grady, MD; Jonathan T. C. Liu, PhD

• ***Context.***—**Anatomic pathologists render diagnosis on tissue samples sectioned onto glass slides and viewed under a bright-field microscope. This approach is destructive to the sample, which can limit its use for ancillary assays that can inform patient management. Furthermore, the subjective interpretation of a relatively small number of 2D tissue sections per sample contributes to low interobserver agreement among pathologists for the assessment (diagnosis and grading) of various lesions.**

Objective.—**To evaluate 3D pathology data sets of thick formalin-fixed Barrett esophagus specimens imaged nondestructively with open-top light-sheet (OTLS) microscopy.**

Design.—**Formalin-fixed, paraffin-embedded Barrett esophagus samples (N = 15) were deparaffinized, stained with a fluorescent analog of hematoxylin-eosin, optically cleared, and imaged nondestructively with OTLS microscopy. The OTLS microscopy images were subsequently compared with archived hematoxylin-eosin histology sections from each sample.**

Results.—**Barrett esophagus samples, both small endoscopic forceps biopsies and endoscopic mucosal resections, exhibited similar resolvable structures between OTLS microscopy and conventional light microscopy with up to a ×20 objective (×200 overall magnification). The 3D histologic images generated by OTLS microscopy can enable improved discrimination of cribriform and well-formed gland morphologies. In addition, a much larger amount of tissue is visualized with OTLS microscopy, which enables improved assessment of clinical specimens exhibiting high spatial heterogeneity.**

Conclusions.—**In esophageal specimens, OTLS microscopy can generate images comparable in quality to conventional light microscopy, with the advantages of providing 3D information for enhanced evaluation of glandular morphologies and enabling much more of the tissue specimen to be visualized nondestructively.**

(*Arch Pathol Lab Med.* doi: 10.5858/arpa.2022-0133-OA)

Esophageal cancers have an estimated annual incidence of more than 19 000 new cases in the United States and carry a poor prognosis, with nearly 15 000 estimated deaths per year for both sexes.[1] The overall incidence of esophageal adenocarcinoma (EAC) is increasing in the United States.[2] Screening and surveillance of the precursor lesion Barrett esophagus (BE) is essential for the prevention of EAC and relies on the detection of dysplasia in BE, which is associated with an increased risk of progression to adenocarcinoma.[3] Assessment of dysplasia in BE is challenging, as evidenced by the poor interobserver agreement among pathologists.[4,5] Despite recent advances in digital 2D whole slide imaging and efforts to standardize benchmark quality criteria,[6,7] interobserver agreement still remains a challenge as diagnoses are based on the subjective interpretation of a limited number of tissue sections.

Light-sheet fluorescence microscopy is an emerging method of nondestructive 3D microscopy of large optically cleared specimens.[8,9] Open-top light-sheet (OTLS) microscopy, in particular, has been specifically developed as a rapid and convenient method for nondestructive slide-free 3D pathology of diverse clinical specimens.[10–14] Recently, OTLS microscopy has been used for 3D pathology of whole prostate biopsies, providing a hematoxylin-eosin (H&E)–like appearance and comparable resolution to conventional slide-based histology while providing additional insights on glandular architecture that have been shown to improve risk stratification for patients with low- to intermediate-risk prostate cancer.[15,16] In addition, OTLS microscopy has been

Accepted for publication August 1, 2022.

From the Departments of Laboratory Medicine and Pathology (Reddi, Liu), Mechanical Engineering (Barner, Gao, Liu), Medicine (Burke, Grady), and Bioengineering (Liu), University of Washington, Seattle; and the Clinical Research Division, Fred Hutchinson Cancer Research Center, Seattle, Washington (Burke, Grady).

The authors acknowledge funding support from the National Cancer Institute (NCI) through R01CA268207 (Liu), the National Institute of Biomedical Imaging and Bioengineering (NIBIB) through R01EB031002 (Liu), and NSF Graduate Research Fellowship DGE-1762114 (Barner). Funding from the NIH: UO1CA152756, RO1-CA220004, P30CA015704, U54CA163060, UO1CA086402, UO1-CA182940, and the Prevent Cancer Foundation was provided to Grady. Funding is also provided by the Cottrell Family Fund and Listwin Foundation to Grady. Any opinions, findings, and conclusions or recommendations expressed in this material are those of the authors and do not necessarily reflect the views of the National Science Foundation, the National Institutes of Health, or the United States Government.

Liu is a cofounder and shareholder of Alpenglow Biosciences, Inc. Grady is an advisory board member for Freenome and Guardant Health. Grady also receives research support from Tempus and LucidDx. The other authors have no relevant financial interest in the products or companies described in this article.

Corresponding author: Deepti Reddi, MD, Department of Laboratory Medicine and Pathology, University of Washington, 1959 NE Pacific St, Box 356100, Seattle, WA 98195 (email: dreddi@uw.edu).

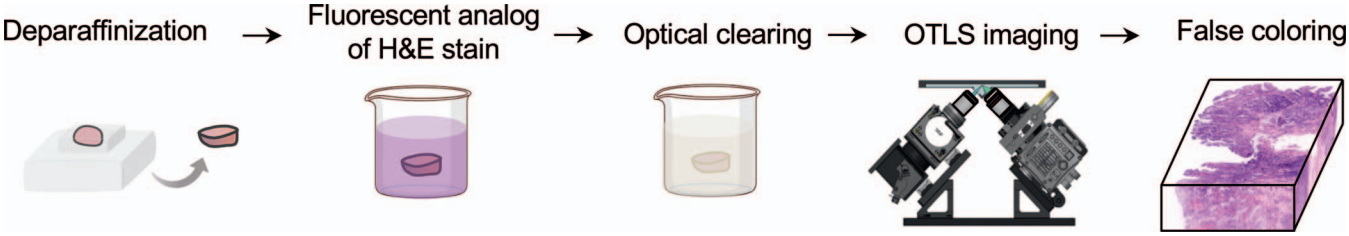

Figure 1. *Flow diagram to summarize the open-top light-sheet (OTLS) microscopy workflow. Abbreviation: H&E, hematoxylin and eosin.*

explored as a potential method for intraoperative assessments of freshly excised breast resection margins.[17]

To demonstrate the potential utility of OTLS microscopy for the evaluation of BE specimens, we present a 3D pathology image atlas of both biopsies and endoscopic mucosal resections (EMRs) from BE patients. In this study, we show a range of both benign and neoplastic histology imaged with OTLS microscopy and provide comparisons with conventional histology. By enabling 3D assessments of large tissue volumes, OTLS microscopy may enhance the assessment of heterogeneous tissue microarchitectures and the cytology of neoplastic glands, which may improve overall diagnostic accuracy, grading of dysplasia, and interobserver agreement.

MATERIALS AND METHODS

Case Selection

Formalin-fixed, paraffin-embedded (FFPE) tissue blocks from BE patients (N = 15 samples from 8 endoscopic biopsies and 7 EMRs), with and without dysplasia, were retrieved from the University of Washington (Seattle) discarded tissue pathology archives. The samples were collected between 2009 and 2018. All patients were consented for tissue donation following protocols approved by the University of Washington Institutional Review Board.

Staining Protocol

FFPE specimens were deparaffinized with incubation at 70°C for 1 hour and subsequent immersion in xylene at 65°C for 48 hours. After deparaffinization, specimens were washed in 100% ethanol for 2 hours and subsequently in 70% ethanol (30% deionized water) for 1 hour. Specimens were stained with an H&E fluorescent analog consisting of TO-PRO-3 Iodide (hematoxylin analog; 1:1000 dilution; Cat. T3605, Thermo-Fisher) and Eosin-Y (1:2000 dilution; Cat. 3801615, Leica Biosystems) in a 70% ethanol (in deionized water) staining buffer at pH 4 (titrated with HCl) with light shaking at room temperature for 48 hours. After staining, specimens were washed in 2 changes of 100% ethanol for 1 hour each. Finally, specimens were optically cleared by immersing in 2 changes of ethyl cinnamate for 2 hours each.[13] After OTLS imaging, the samples were immersed in 100% ethanol for 2 hours and in xylene for 1 hour, and then re-embedded in paraffin.

OTLS Microscopy

After fluorescent staining and optical clearing, specimens were mounted on a flat sample holder (Hivex material, refractive index $n = 1.56$) and imaged in 3D with a previously reported "third-generation" OTLS microscope.[11] Specimens were illuminated with a light sheet (numerical aperture approximately 0.09) using laser wavelengths of 660 and 488 nm to excite TO-PRO-3 and Eosin-Y, respectively. Fluorescence was collected with a ×20 collection objective, filtered by a band-pass filter (LP02-664RU-25 and FF1-496/LP-25, Semrock), then relayed by a tube lens onto a scientific complementary metal oxide semiconductor camera (ORCA-Flash4.0 V2, Hamamatsu). The lateral and axial resolutions achieved were approximately 0.65 and 2.75 μm, respectively.[11] Specimens were scanned at a rate of approximately 0.03 mm^3/min and the volumetric data sets were compressed by approximately ×10 using B3D compression.[18] Each image was stored in a hierarchical data format (HDF5) and false colored to mimic conventional H&E staining using a Python-based algorithm described by Serafin et al.[19] For the bright exogenously labeled specimens imaged in this study, photobleaching was not observed. A summary of the imaging workflow (ie, tissue preparation, imaging, and postprocessing) is provided in Figure 1.

Histologic Examination

H&E-stained slides were obtained from pathology archives for each tissue sample and scanned at ×40 magnification to produce a whole slide image (Aperio, Leica Biosystems). A board-certified gastrointestinal pathologist reviewed each case.

RESULTS

Normal and Metaplastic Structures

As part of the recommended care of patients with BE, surveillance upper endoscopy with forceps biopsies of the involved segment of the esophagus is performed every 1 to 3 years. Four-quadrant biopsies are obtained every 1 to 2 cm along the length of the BE.[20] Figure 2, A through D, highlights normal structures seen in OTLS microscopy of endoscopic biopsies (with H&E false coloring) in comparison with corresponding standard H&E histology. With both OTLS microscopy and standard histology, lymphocytes are seen in the squamous epithelium as small cells with dark nuclei (black arrows), and rete pegs are apparent with blood vessels containing red blood cells (white arrows), shown in Figure 2, A and B. Nondysplastic columnar (cardiac) mucosa is seen with apical gastric-type mucin vacuoles and basally oriented nuclei, shown in Figure 2, C and D.

BE is a precursor lesion to EAC and is defined as replacement of the squamous epithelium by a metaplastic columnar epithelium with goblet cells.[6] The goblet cells contain clear to blue cytoplasmic mucin with indented nuclei, as is apparent in Figure 3, A through D, for both OTLS microscopy and conventional histology. Of note, there are several artifacts encountered in conventional histology evaluation due to fixation, tissue processing, embedding, and microtomy, which impair the ability of the pathologist to interpret the tissue samples.[21] For example, in Figure 3, D, tissue fractures ("chatter" artifacts) created during microtome sectioning are apparent, but OTLS images of the same specimen do not exhibit such artifacts (Figure 3, C).

Low- and High-Grade Intestinal Dysplasia

In patients with dysplastic BE, EMR is commonly performed to treat the dysplastic BE and to improve diagnosis and staging. These large specimens improve the interobserver agreement among pathologists compared with small endoscopic forceps-biopsy specimens.[22] An

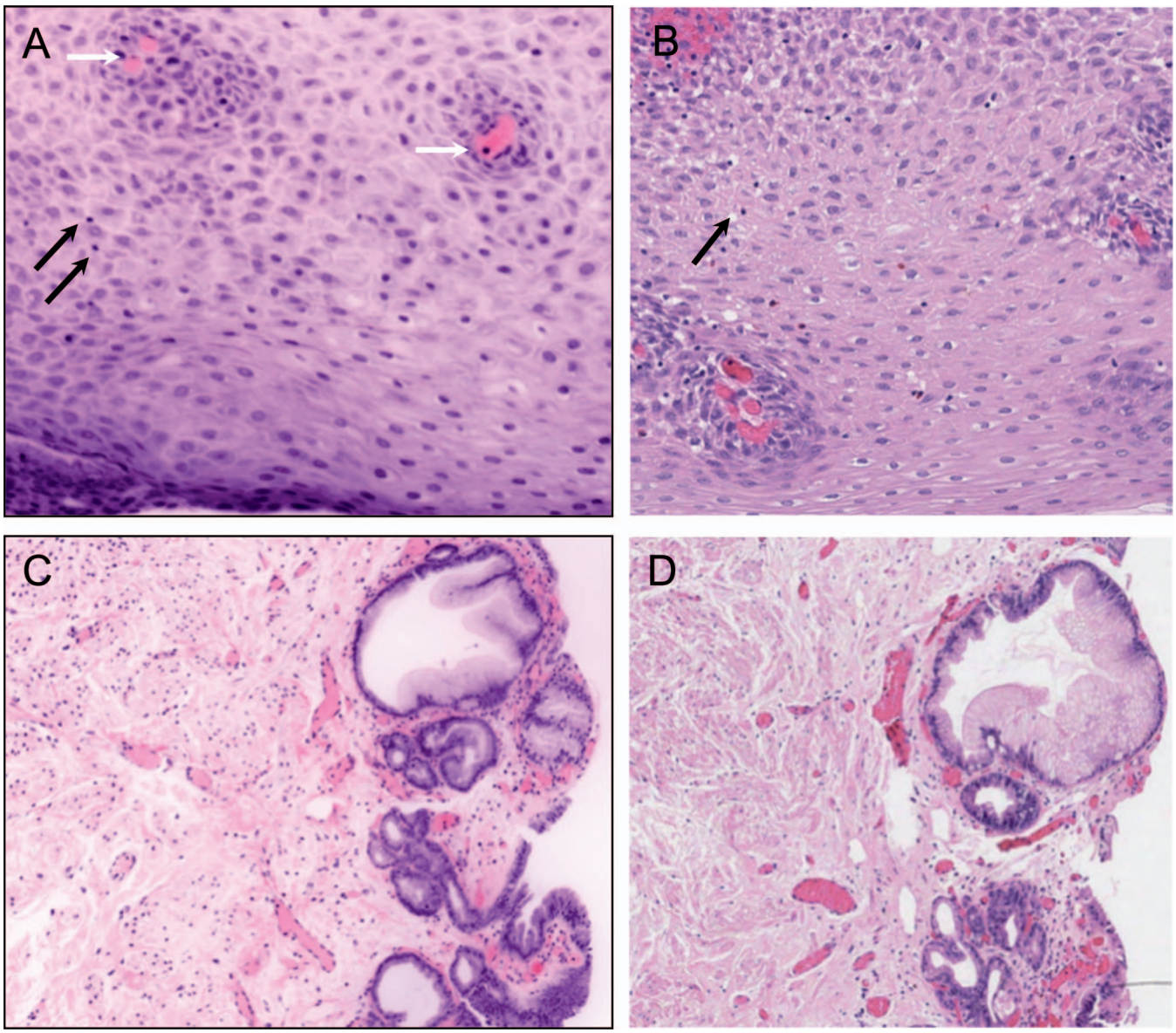

Figure 2. *Normal histologic structures in endoscopic mucosal resections. A, Open-top light-sheet (OTLS) microscopy view of the squamous epithelium with intraepithelial lymphocytes (black arrows) and rete pegs (white arrows). B, Standard histology showing focal areas of spongiosis and intraepithelial lymphocytes (black arrow). C, OTLS view of the cardiac/columnar mucosa with gastric-type apical mucin vacuoles. D, Standard histology of the same region shows no evidence of goblet cells or dysplasia (hematoxylin-eosin false colored, original magnification ×20 [A and C]; hematoxylin-eosin, original magnification ×10 [B and D]).*

example of a nondysplastic esophageal specimen is shown in the full-thickness section in Figure 4, A and B, in OTLS and conventional histology, with layers of mucosa, muscularis mucosa, and submucosa. Of note, thickening of the muscularis mucosa by smooth muscle hypertrophy is seen in patients with BE because of chronic inflammation and prior endoscopic procedural injury.[23] Another example of a full-thickness section of BE with low-grade dysplasia (LGD) (top inset) is shown in Figure 5, A and B, in OTLS and conventional histology, with a discontinuous muscularis mucosa and prominent submucosal glands (bottom inset) in the submucosa.

In patients with dysplastic BE, the accurate assessment of the grade of the dysplasia dictates patient management. Most glandular dysplasia in the esophagus is of the intestinal type, which is graded as LGD or high-grade dysplasia (HGD) based on cytologic atypia and architectural complexity. In Figure 6, A and B, there is LGD extending to the surface epithelium with loss of mucin and goblet cells, shown with OTLS microscopy and standard histology, respectively. The nuclei are hyperchromatic with focal areas of increased mitosis. HGD is shown in Figure 6, C and D, with increased crowding and focal areas of cribriform glands and luminal necrosis (circle). OTLS images are similar in quality to conventional histology, but with the advantage of enabling 3D evaluation of glandular structure.

In this initial study with OTLS microscopy of human esophagus specimens, we have shown that 3D structural information of neoplastic glands could potentially improve the accuracy of grading dysplastic regions. This is of importance because the grade of dysplasia impacts the

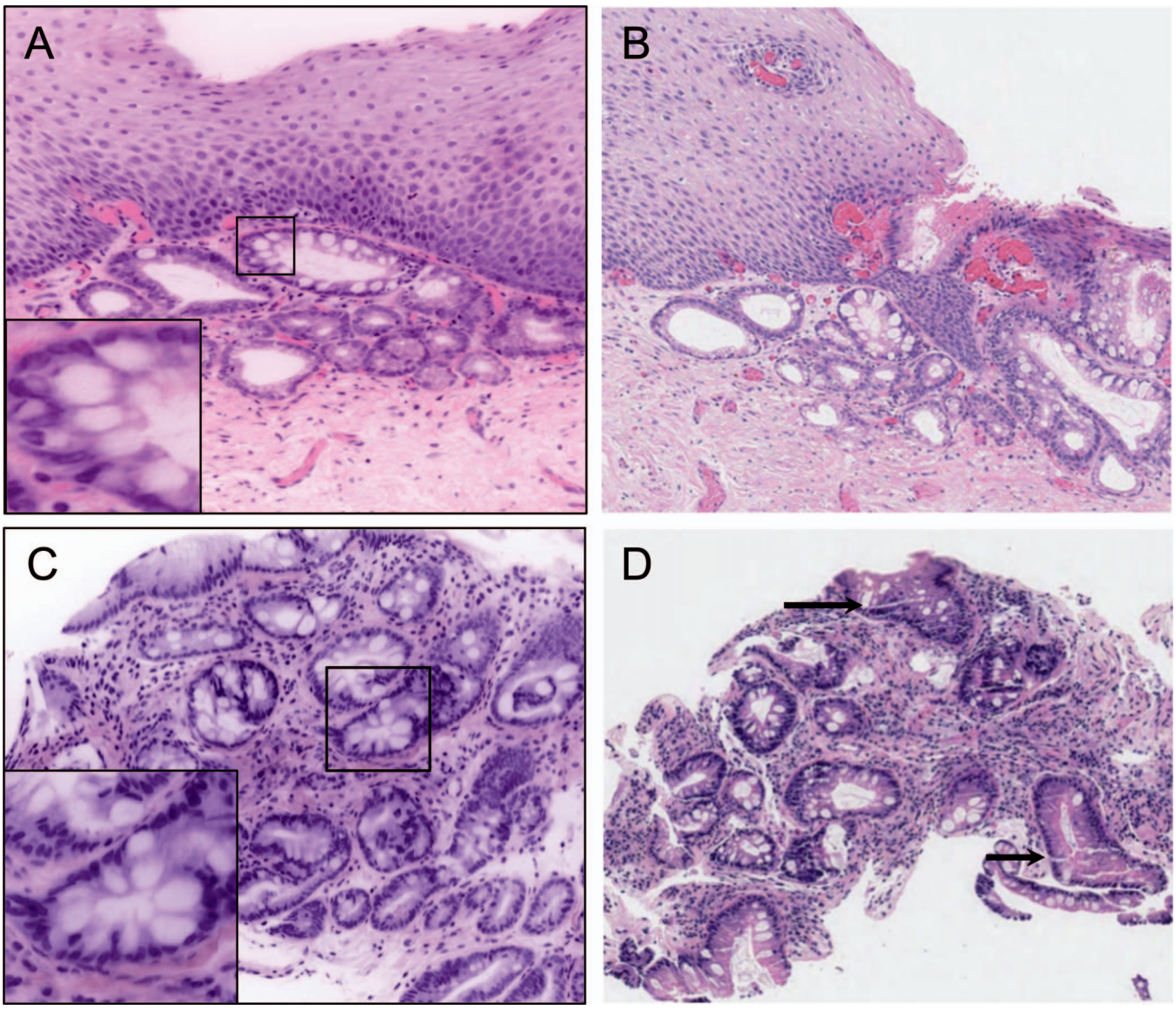

Figure 3. *Goblet cell metaplasia (Barrett esophagus) in an endoscopic mucosal resection and biopsy. A and B, An endoscopic mucosal resection with squamocolumnar junction is shown with open-top light-sheet (OTLS) microscopy (A and inset) and standard histology (B), respectively. C and D, A biopsy specimen evaluated by OTLS (C) exhibits no artifacts whereas standard histology shows tissue fractures (arrows) generated during tissue sectioning and slide preparation (D). C inset, magnified OTLS view of the goblet cells with peripheral nuclei (hematoxylin-eosin false colored, original magnification ×20 [A, A inset, C, and C inset]; hematoxylin-eosin, original magnification ×10 [B and D]).*

decision to proceed to endoscopic eradication therapy (common for HGD) or active surveillance (common for LGD).[24] In our pilot study, one biopsy was originally diagnosed as LGD based on standard histology. However, subsequent evaluation of the entire remaining biopsy tissue by OTLS microscopy revealed focal areas that could be indicative of HGD. For example, a sequence of images at various depths within the specimen is shown in Figure 7, A and B. A pair of glands that appear distinct at the surface of the specimen appear to fuse at other depths (30 and 60 μm deep), which is a feature associated with HGD. In Figure 7, C through E, OTLS microscopy images reveal some high-grade nuclear features with nucleoli and increased mitosis toward the gland lumen, supporting nuclear stratification with loss of polarity. The complex architectural and cytologic features observed could contribute in upgrading to HGD. Figure 7, F, shows a whole slide image of the original H&E histology section used to diagnose this biopsy as LGD rather than HGD. Interestingly, patient records showed that an EMR was performed a month after this biopsy, and that the EMR specimen was diagnosed as HGD, thereby confirming our OTLS-based findings from imaging the initial biopsy.

In summary, because of the limited sampling of endoscopic biopsies via standard slide-based histology, in which only a few thin 2D tissue sections are visualized, focal regions of higher-grade pathology may be missed. However, comprehensive interrogation of biopsies with nondestructive 3D pathology can help to identify such focal regions (ie, "rare events"), as enabled by OTLS microscopy in this case. Furthermore, 3D pathology can enable improved characterization of complex and heterogeneous 3D structures, such as glands that may fuse and become cribriform as they migrate spatially.

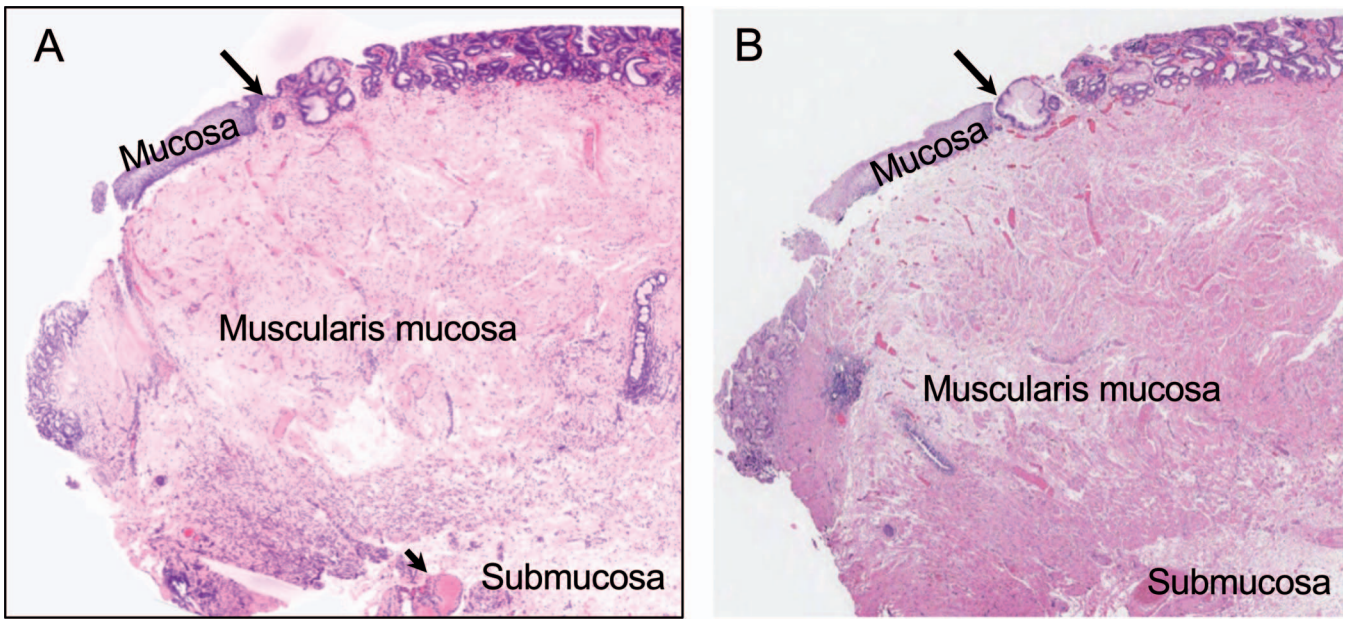

Figure 4. *Full-thickness section of an endoscopic mucosal resection showing nondysplastic Barrett esophagus. A, Open-top light-sheet microscopy with labels for the mucosa with the gastroesophageal junction (arrow), a thickened muscularis mucosa, and the submucosa exhibiting thick vessels (arrowhead). B, Corresponding standard histology image showing the same structures (hematoxylin-eosin false colored, original magnification ×20 [A]; hematoxylin-eosin, original magnification ×2 [B]).*

DISCUSSION

In anatomic pathology, gastrointestinal and gynecologic specimens are reported as having the highest rates of inaccurate diagnoses and interobserver discordance.[25] Major discordance in diagnosis occurs because of the subjective element of the diagnostic process, as well as inherent sampling limitations, ambiguities, and artifacts that arise from viewing thin 2D tissue sections. Evaluation of the presence and grade of dysplasia in BE is associated with substantial interobserver variability, especially with evaluation of dysplasia.[26] In an attempt to mitigate these limitations, gastroenterologists perform repeat endoscopy within 3 to 6 months of an initial BE diagnosis to confirm the diagnosis before making the decision to proceed with endoscopic therapy or surveillance. Our long-term hypothesis is that examining biopsy and resection specimens with

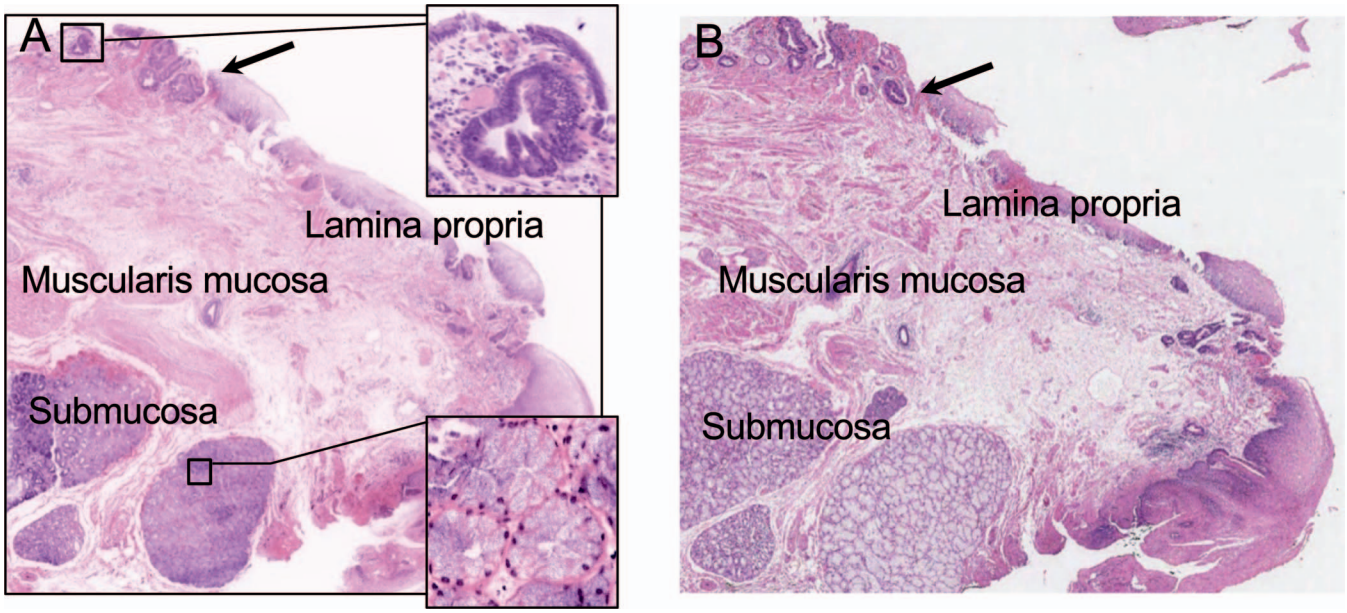

Figure 5. *Full-thickness section of dysplastic Barrett esophagus in an endoscopic mucosal resection. A, Open-top light-sheet view of the resection specimen in which the gastroesophageal junction is labeled with an arrow. The 3 layers of the esophagus are also labeled: the mucosa, a thin discontinuous muscularis mucosa, and the submucosa with prominent submucosal glands. The top inset shows overlying low-grade dysplasia and the bottom inset shows mucinous submucosal glands. B, Standard histology shows the same structures (hematoxylin-eosin false colored, original magnification ×20 [A]; hematoxylin-eosin, original magnification ×2 [B]).*

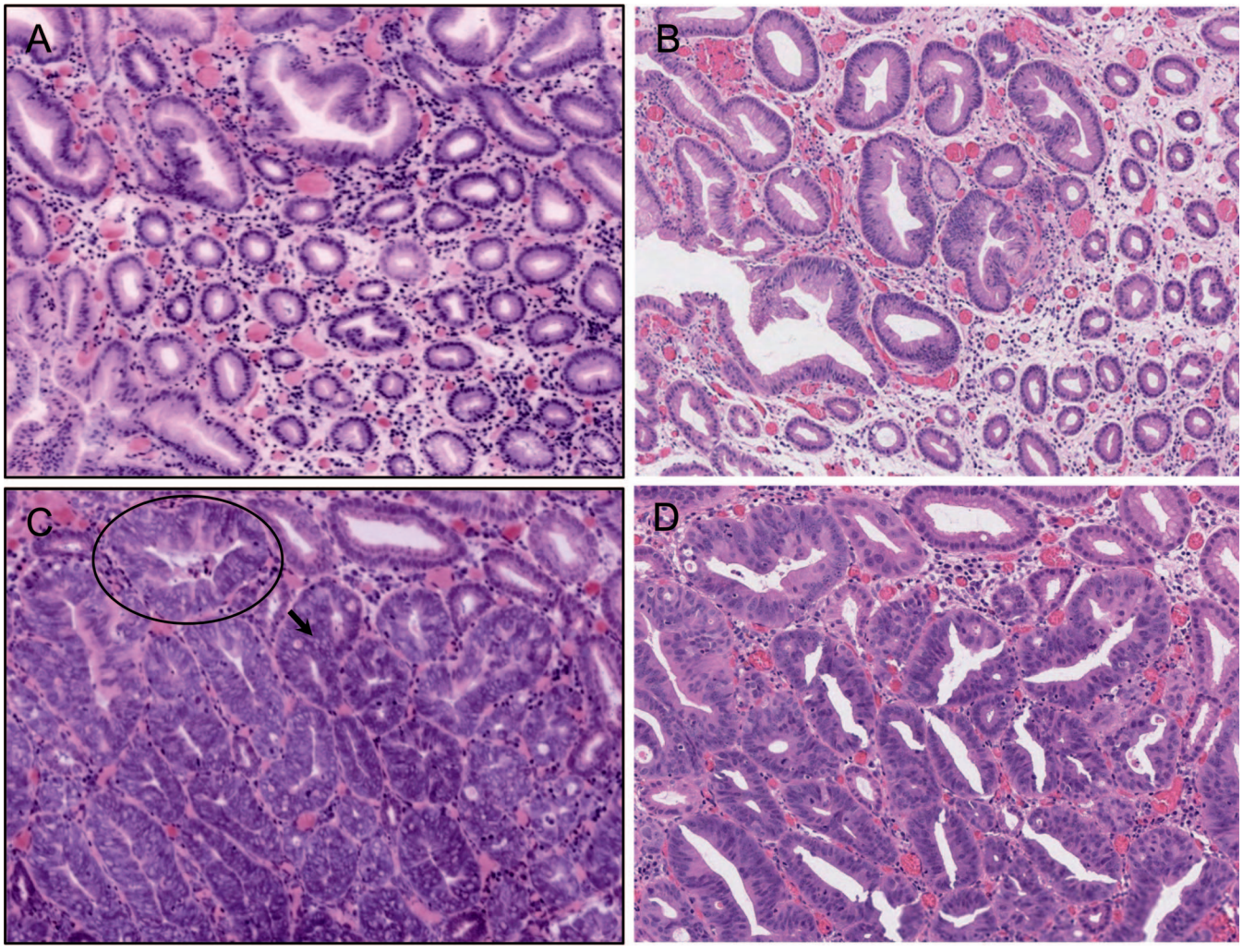

Figure 6. *Dysplastic Barrett esophagus in endoscopic mucosal resections. A and B, An abrupt transition to low-grade dysplasia, shown on upper left side, with nuclear hyperchromasia and increased mitosis, seen with both open-top light-sheet (OTLS) microscopy and standard histology, respectively. C and D, Areas of high-grade dysplasia with cribriform glands (arrow) and luminal necrosis (circle), seen with both OTLS microscopy and standard histology, respectively (hematoxylin-eosin false colored, original magnification ×20 [A and C]; hematoxylin-eosin, original magnification ×10 [B and D]).*

3D pathology may improve diagnostic accuracy and interobserver agreement because of the vastly greater amount of tissue that can be examined nondestructively, as well as the ability to more clearly characterize complex 3D structures (eg, glands) that are of diagnostic and prognostic importance. Further studies are necessary to examine this hypothesis, including quantification of intraobserver and interobserver variability with OTLS microscopy (compared with conventional 2D histology), as well as the ability to improve prognostic accuracy. In addition, we are training artificial intelligence–based classifiers to help with prognostication using 3D pathology data sets. All of these studies will require larger, well-curated patient cohorts paired with clinical outcomes.

Along with OTLS microscopy, there are other emerging slide-free technologies, such as multiphoton microscopy,[27] stimulated Raman spectroscopy,[28,29] microscopy with ultraviolet surface excitation,[30,31] structured illumination,[32] and confocal microscopy.[33] These technologies avoid histologic artifacts that result from poor fixation, thick sectioning, folds and tears, and staining variability. However, light-sheet microscopy has emerged as a particularly powerful method to image large thick-tissue specimens provided that they are optically cleared to render them transparent to light.[8,9] When tissues are optically cleared well, high image quality can be maintained to a depth of many millimeters and even centimeters, as for example demonstrated with a more recent OTLS microscope system with a 1-cm working distance.[14]

Among light-sheet microscopy techniques, OTLS microscopy has been designed specifically for applications in anatomic pathology and is a versatile technology for a broad range of specimens and clinical applications, including both rapid imaging of freshly excised tissue surfaces and deep volumetric microscopy of optically cleared biopsies and resection specimens. It is also notable that the optical-clearing and fluorescent labeling protocols used in this study are relatively simple, are reversible (ie, tissues can be re-embedded in paraffin), and do not interfere with subsequent slide-based histology methods (eg, H&E, immunohistochemistry, fluorescence in situ hybridization).[11,13,15,17] In fact, the chemicals used for deparaffinization (xylene) and

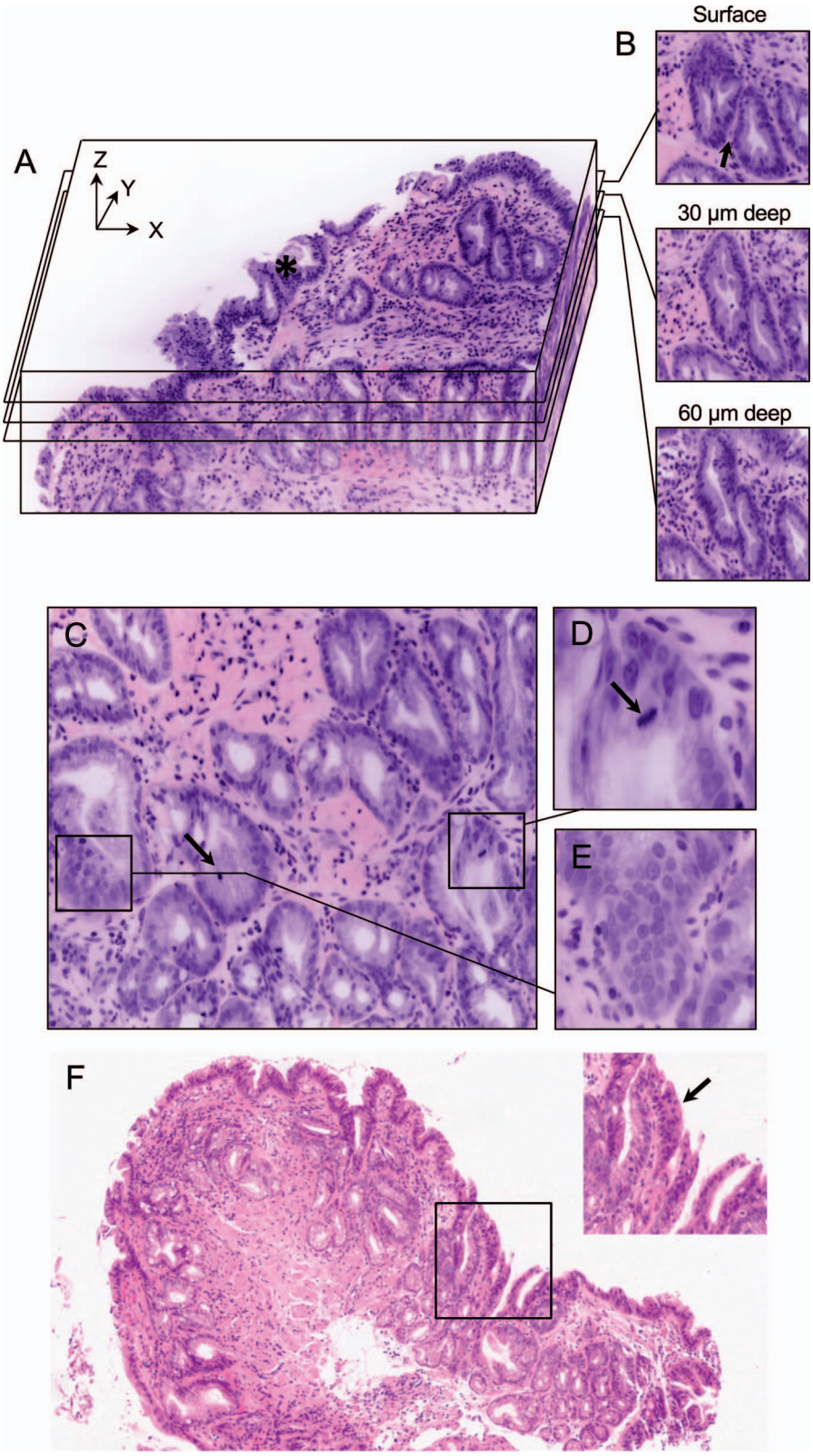

Figure 7. *Comprehensive sampling with open-top light-sheet (OTLS) microscopy reveals architectural features of high-grade dysplasia (HGD) in a biopsy originally diagnosed as low-grade dysplasia (LGD) by conventional histology. A, 3D OTLS data set showing dysplasia extending to the surface epithelium (asterisk). B, 3D pathology enables more accurate assessment of complex glandular structures. An image near the surface of the biopsy (top) displays distinct dysplastic glands with intervening lamina propria (black arrow). However, images deeper within the specimen (middle and bottom right) show that the glands start to fuse with a cribriform architecture (no intervening lamina propria), which is associated with HGD. C through E, OTLS images are shown of a region of interest with neoplastic glands exhibiting nuclear stratification with loss of polarity, inconspicuous nuclei and mitoses extending to the luminal surface (arrows). F, Whole slide image of the original hematoxylin-eosin section that was used for a clinical diagnosis of LGD for this biopsy. The surface epithelium shows nuclear stratification (arrow), high nuclear to cytoplasmic ratio, and increased mitosis, supporting the original diagnosis of LGD with no evidence of architectural complexity (hematoxylin-eosin false colored, original magnification ×20 [A through E]; hematoxylin-eosin, original magnification ×10 [F] and ×20 [F inset]).*

dehydration of tissues (ethanol) are the same chemicals used for the standard-of-care processing of clinical specimens as FFPE blocks. Of note, the optical sectioning of the OTLS microscope in this study (slightly less than 4 µm in thickness) is similar to that of standard histology sections, which allows for the generation of images that are comparable in appearance to standard histology. However, because nondestructive OTLS microscopy images do not exhibit certain artifacts of conventional histology, such as shrinkage-induced cracks and voids between cells and tissue structures, this could affect diagnostic determinations for pathologists accustomed to standard FFPE histology.

A limitation of our study is that all the OTLS images in this study were obtained with a ×20 objective. For ×40- and ×60-equivalent resolution, a newer OTLS microscope has recently been developed.[14] Another limitation of our pilot study of 15 BE samples is that we did not study large resections such as endoscopic mucosal dissections and esophagectomy specimens that are used for accurate pathologic tumor node metastasis staging of esophageal carcinoma.[34] In the future, we would like to examine such specimens to evaluate the potential of OTLS microscopy to improve these staging paradigms. We would also like to include information about specimen orientation by imaging the surgical ink applied during gross specimen evaluation, which is essential for determining tissue-margin status but was not imaged with OTLS microscopy in this study. It is also important to realize that there will be a learning curve for pathologists when evaluating comprehensive 3D data sets (as opposed to 2D images from conventional histology), which may be facilitated by the implementation of user-friendly software for visualizing 3D data and artificial intelligence–based image-screening tools. Well-powered and controlled clinical studies are needed to determine the clinical utility of 3D pathology of BE specimens and whether/how it can improve interobserver concordance and accuracy for diagnosis and grading. Future studies could also assess the use of 3D OTLS microscopy in conjunction with molecular markers for tumor suppressor genes, oncogenes, and aneuploidy to improve clinical decision-making for BE patients.

In addition to providing feature-rich 3D information over large volumes of tissue (eg, whole biopsies), OTLS microscopy has a number of practical benefits for clinical laboratories, such as being nondestructive of valuable clinical specimens and obviating the need for highly skilled histotechnologists (as needed for high-quality microtome sectioning). However, a number of major challenges need to be overcome in order to facilitate clinical adoption, as discussed in a recent perspective review.[9] Perhaps the greatest challenge is in handling the massive data sets that 3D pathology techniques generate and analyzing them in a data- and time-efficient manner. Computational tools will almost certainly be necessary to guide pathologists to the most important regions for visual interpretation, as well as to provide automated decision support based on both intuitive (ie, "handcrafted") and abstract (ie, deep learning–derived) features.

In conclusion, 3D pathology enabled by OTLS microscopy can enable the comprehensive nondestructive examination of large clinical specimens, thereby generating large amounts of feature-rich volumetric data for human and/or computational analysis. This technology has the potential to improve diagnostic/prognostic accuracy and to improve patient care.

References

1. Siegel RL, Miller KD, Fuchs HE, Jemal A. Cancer statistics, 2021. *CA Cancer J Clin*. 2021;71(1):7–33.

2. Domper Arnal MJ, Ferrández Arenas Á, Lanas Arbeloa Á. Esophageal cancer: risk factors, screening and endoscopic treatment in Western and Eastern countries. *World J Gastroenterol*. 2015;21(26):7933–7943.

3. Waters KM, Salimian KJ, Voltaggio L, Montgomery EA. Refined criteria for separating low-grade dysplasia and nondysplastic Barrett esophagus reduce equivocal diagnoses and improve prediction of patient outcome: a 10-year review. *Am J Surg Pathol*. 2018;42(12):1723–1729.

4. Kerkhof M, van Dekken H, Steyerberg EW, et al. Grading of dysplasia in Barrett's oesophagus: substantial interobserver variation between general and gastrointestinal pathologists. *Histopathology*. 2007;50(7):920–927.

5. Coco DP, Goldblum JR, Hornick JL, et al. Interobserver variability in the diagnosis of crypt dysplasia in Barrett esophagus. *Am J Surg Pathol*. 2011;35(1):45–54.

6. van der Wel MJ, Duits LC, Seldenrijk CA, et al. Digital microscopy as valid alternative to conventional microscopy for histological evaluation of Barrett's esophagus biopsies. *Dis Esophagus*. 2017;30(11):1–7.

7. van der Wel MJ, Klaver E, Duits LC, et al. Adherence to pre-set benchmark quality criteria to qualify as expert assessor of dysplasia in Barrett's esophagus biopsies—towards digital review of Barrett's esophagus. *United European Gastroenterol J*. 2019;7(7):889–896.

8. Stelzer EHK, Strobl F, Chang BJ, et al. Light sheet fluorescence microscopy. *Nat Rev Methods Primers*. 2021;1:73. doi:10.1038/s43586-021-00069-4

9. Liu JTC, Glaser AK, Bera K, et al. Harnessing non-destructive 3D pathology. *Nat Biomed Eng*. 2021;5(3):203–218.

10. Glaser AK, Reder NP, Chen Y, et al. Light-sheet microscopy for slide-free non-destructive pathology of large clinical specimens. *Nat Biomed Eng*. 2017;1(7):0084.

11. Barner LA, Glaser AK, Huang H, True LD, Liu JTC. Multi-resolution open-top light-sheet microscopy to enable efficient 3D pathology workflows. *Biomed Opt Express*. 2020;11(11):6605–6619.

12. Barner LA, Glaser AK, True LD, Reder NP, Liu JTC. Solid immersion meniscus lens (SIMlens) for open-top light-sheet microscopy. *Opt Lett*. 2019;44(18):4451–4454.

13. Glaser AK, Reder NP, Chen Y, et al. Multi-immersion open-top light-sheet microscope for high-throughput imaging of cleared tissues. *Nat Commun*. 2019;10(1):2781.

14. Glaser AK, Bishop KW, Barner LA, et al. A hybrid open-top light-sheet microscope for versatile multi-scale imaging of cleared tissues. *Nat Methods*. 2022;19(5):613–619.

15. Reder NP, Glaser AK, McCarty EF, Chen Y, True LD, Liu JTC. Open-top light-sheet microscopy image atlas of prostate core needle biopsies. *Arch Pathol Lab Med*. 2019;143(9):1069–1075.

16. Xie W, Reder NP, Koyuncu C, et al. Prostate cancer risk stratification via nondestructive 3D pathology with deep learning-assisted gland analysis. *Cancer Res*. 2022;82(2):334–345.

17. Chen Y, Xie W, Glaser AK, et al. Rapid pathology of lumpectomy margins with open-top light-sheet (OTLS) microscopy. *Biomed Opt Express*. 2019;10(3):1257–1272.

18. Balazs B, Deschamps J, Albert, M, Ries J, Hufnagel L. A real-time compression library for microscopy images [published online July 21, 2017]. *bioRxiv*. doi:10.1101/164624

19. Serafin R, Xie W, Glaser AK, Liu JTC. FalseColor-Python: a rapid intensity-leveling and digital-staining package for fluorescence-based slide-free digital pathology. *PLoS One*. 2020;15(10):e0233198.

20. Shaheen NJ, Falk GW, Iyer PG, Gerson LB; American College of Gastroenterology. ACG clinical guideline: diagnosis and management of Barrett's esophagus. *Am J Gastroenterol*. 2016;111(1):30–51.

21. Taqi SA, Sami SA, Sami LB, Zaki SA. A review of artifacts in histopathology. *J Oral Maxillofac Pathol*. 2018;22(2):279.

22. Wani S, Mathur SC, Curvers WL, et al. Greater interobserver agreement by endoscopic mucosal resection than biopsy samples in Barrett's dysplasia. *Clin Gastroenterol Hepatol*. 2010;8(9):783–788.

23. Lewis JT, Wang KK, Abraham SC. Muscularis mucosae duplication and the musculo-fibrous anomaly in endoscopic mucosal resections for Barrett esophagus: implications for staging of adenocarcinoma. *Am J Surg Pathol*. 2008;32(4):566–571.

24. Sharma P, Shaheen NJ, Katzka D, Bergman JJGHM. AGA Clinical practice update on endoscopic treatment of Barrett's esophagus with dysplasia and/or early cancer: expert review. *Gastroenterology*. 2020;158(3):760–769.

25. Peck M, Moffat D, Latham B, Badrick T. Review of diagnostic error in anatomical pathology and the role and value of second opinions in error prevention. *J Clin Pathol*. 2018;71(11):995–1000.

26. Curvers WL, ten Kate FJ, Krishnadath KK, et al. Low-grade dysplasia in Barrett's esophagus: overdiagnosed and underestimated. *Am J Gastroenterol*. 2010;105(7):1523–1530.

27. Torres R, Olson E, Homer R, et al. Initial evaluation of rapid, direct-to-digital prostate biopsy pathology. *Arch Pathol Lab Med*. 2021;145(5):583–591.

28. Hollon TC, Pandian B, Adapa AR, et al. Near real-time intraoperative brain tumor diagnosis using stimulated Raman histology and deep neural networks. *Nat Med*. 2020; 26 (1): 52–58.

29. Zhang L, Wu Y, Zheng B, et al. Rapid histology of laryngeal squamous cell carcinoma with deep-learning based stimulated Raman scattering microscopy. *Theranostics*. 2019; 9 (9): 2541–2554.

30. Fereidouni F, Harmany ZT, Tian M, et al. Microscopy with ultraviolet surface excitation for rapid slide-free histology. *Nat Biomed Eng*. 2017;1:957–966.

31. Yoshitake T, Giacomelli MG, Quintana LM, et al. Rapid histopathological imaging of skin and breast cancer surgical specimens using immersion microscopy with ultraviolet surface excitation. *Sci Rep*. 2018;8(1):4476.

32. Wang M, Tulman DB, Sholl AB, et al. Gigapixel surface imaging of radical prostatectomy specimens for comprehensive detection of cancer-positive surgical margins using structured illumination microscopy. *Sci Rep*. 2016;6:27419.

33. Abeytunge S, Li Y, Larson B, et al. Confocal microscopy with strip mosaicing for rapid imaging over large areas of excised tissue. *J Biomed Opt*. 2013;18(6):61227.

34. Amin MB, Edge SB, Greene FL, et al, eds. *AJCC Cancer Staging Manual*. 8th ed. New York, NY: Springer; 2017.